

SF₆ Gas Insulation for next Generation GIS

Fumihito Endo

Hitachi Ltd., Power & Industry Systems R&D Division
7-2-1 Omika-cho, Hitachi-shi, Ibaraki-ken, 319-1221 Japan

Abstract

Many factors influence SF₆ insulation and a number of them have been clarified quantitatively. For the next generation of gas-insulated switchgear (GIS), quantitative considerations of these factors are necessary to enhance reliability and to make GIS more compact. Advanced insulation technology for this purpose is described.

INTRODUCTION

Thirty years have past since the first application of GIS to bulk power transmission systems. In this period, SF₆ gas insulation technology has undergone much development, not only of the insulation itself, but also of the GIS technology, including its quality control, diagnostic systems, dielectric materials, test technique and so on. Owing to this development, UHV (1100 kV) GIS, new 550 kV compact GIS and DC 500 kV GIS have successfully been appeared [1,2,3].

This paper introduces key insulation technology of new generation GIS.

INSULATION DESIGN PROCEDURE

Next generation GIS is characterized by greater compactness and higher reliability. Knowledge of high voltage engineering and manufacturing processes is essential for such GIS, with the former including knowledge of insulation characteristics, materials, insulation diagnosis, insulation coordination, etc., and the latter including knowledge of design, quality control, test techniques, preventive maintenance, etc.

Table 1 shows typical procedures for next generation GIS. To get better reliability and compactness at the same time, it is necessary to accurately predict insulation strength under both normal and abnormal conditions. With such a prediction, it is possible to optimize the insulation structure. To assure GIS quality, factory and site tests play an important role, and are supported by a new highly sensitive partial discharge (PD) diagnostic system.

Table 1. Typical procedures to enhance reliability of GIS.

stage	procedures
design	(1) suitable insulation structures (2) proper insulation margin (3) consideration for factors decreasing reliability such as particles, voltage wave shapes etc. (4) prediction of breakdown voltages
manufacturing	quality control for particles, protrusions, defects etc.
factory test	(1) AC, IMP and/or DC tests (2) highly-sensitive PD diagnosis
site test	(1) AC and Osc. LI tests (2) high S/N PD diagnosis

FACTORS TO INFLUENCE GAS INSULATION

Gas insulation is influenced by many factors. Typical ones are shown in Fig. 1. A short gap between a shield and an insulator is usually no problem for AC and impulse voltages, but for DC voltages it often seriously affects insulation strength. Electric potential distribution of an insulator is determined by its resistivity, and potential difference between the edge of a shield and an insulator becomes larger as distance L is longer. Then field intensity at gap g increases. This phenomenon is quite different from that in an AC case. Local concentration of an electric field at triple junctions sometimes decreases surface breakdown voltages of spacers as well as field concentration on a spacer surface. A high voltage shield to mitigate electric field at a triple junction has a potential to become a source for field emission and partial discharges, and it can cause charge accumulation on a spacer. Conducting particles greatly decrease breakdown voltages. Analysis of their motion analysis and estimation of breakdown voltages are very important.

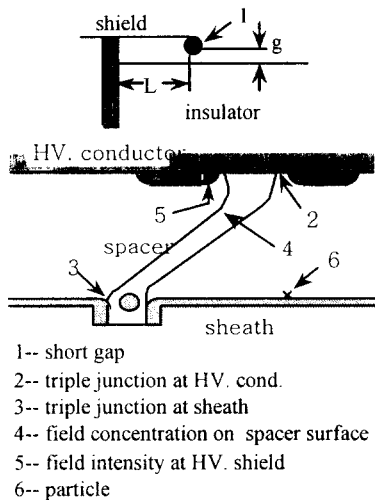


Fig. 1. Factors to be considered in insulation performance.

TRIPLE JUNCTION

At a triple junction on a spacer, the electric field at a micro gap is intensified and the magnitude of discharges generated there changes as shown in Fig. 2(a). Discharges initiate at relatively low voltages and breakdown occurs when the streamer criterion in eq.(1) is satisfied.

$$\text{eff } dz = \text{const.} \quad (1)$$

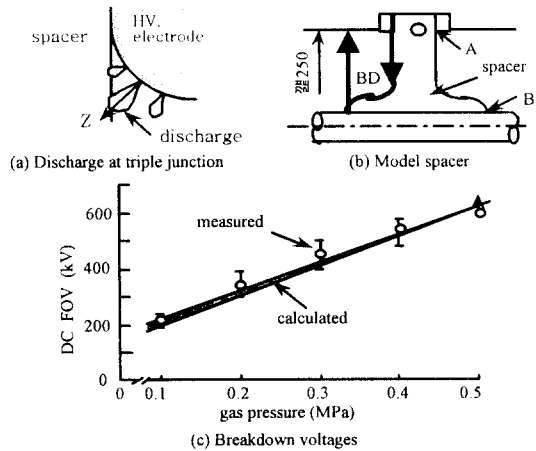


Fig. 2. Breakdown at triple junction.

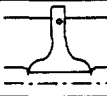
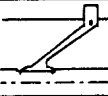
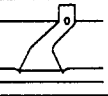
Where eff , effective ionization coefficient; z , distance from a high voltage electrode.

In previous papers [4, 5], good agreement between calculated and measured values was reported in the lightning impulse case. For the DC case, breakdown voltages were measured with disc spacers of 250 mm dia. in Fig. 2(b) and they are plotted in Fig. 2(c). Breakdowns originated at triple junctions at both points A and B. The streamer criterion in eq. (1) was applied at both triple junctions, and calculated values are shown as solid lines. In this DC case, calculated values agreed fairly well with measured ones. Good agreement was confirmed for other types of spacers. From the calculation, it became possible to design the optimum shield structures such as a dielectric shield, an insert shield and an outer shield [5] for both AC and DC GIS.

SPACER

Various surges travel to, and are generated in, GIS. A spacer has to withstand all of these surges. Basic insulation strength is specified in international and national standards. However, in modern trunk power net works some considerations should be added to the standards. Veryfasttransientover-voltages(VFT) and trapped residual DC voltages are typical cases. Insulation strength for VFT is dominated by maximum field intensity E_m as well as lightning impulse voltages. Charge accumulation of a spacer by residual DC voltages is dependent on normal field component E_n . On the other hand, particle-initiated breakdown voltages are determined by tangential field component E_t . It is desirable to minimize these three field components. Each component is compared in Table 2 [5]. A disc spacer has low E_n and medium E_m , and a cone one has low E_t . A hybrid cone spacer has merits of both types of spacers. Further optimization by changing angles of each taper and bending position of the concave surface gives a hybrid spacer for which very high insulation strength can be obtained. Fig. 3 shows an example of optimized spacer. This spacer had excellent insulation performance for various voltage shapes including DC under both clean and contaminated conditions [3, 6].

Table 2. Comparison of field intensity of spacers.

	disc	cone	hybrid cone
spacer shape			
E_m	M	H	L
E_t	H	L	M
E_n	L	H	L

H: high, M: medium, L: low

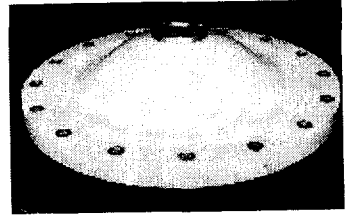


Fig. 3. Optimized hybrid cone spacer.

PARTICLES

Metallic particles move up and down owing to electrostatic force and gravity. Their motion is described by eq. (2),

$$m \frac{d^2 \mathbf{x}}{dt^2} = Q\mathbf{E} + m\mathbf{g} + \mathbf{F}_d \quad (2)$$

where \mathbf{x} , particle position; \mathbf{E} , electric field; m and Q , mass and electric charge of a particle; and \mathbf{F}_d , drag force. As GIS structure is usually unsymmetric with respect to an axis of a bus, distribution of \mathbf{E} becomes three-dimensional and must be calculated with a three-dimensional field analysis program. By combining eq. (2) with such a program, particle motion can be calculated exactly. An example simulation is shown in Fig.4 [7]. A concentric cylindrical electrode of 300 mm dia. had a particle trap of 100 mm dia. at the bottom of the outer electrode. A 5 mm long particle of 0.25 mm dia. was dropped from the inner electrode. The particle repeated a three-dimensional bounce, and finally dropped into the trap.

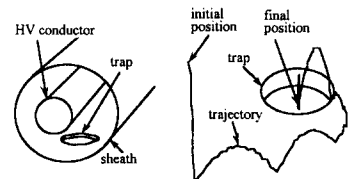


Fig. 4. Three-dimensional motion simulation of a 5mm long aluminum particle ; concentric cylinder electrode of 80/300 mm dia.

Particle-initiated breakdown voltages are greatly influenced by particle position. A typical example of surface breakdowns is shown in Fig. 5. Five mm long particles were attached on the surface of an 80 mm high post spacer, and breakdown voltages were measured by changing attachment position. Breakdown voltages changed for particle position. As particle motion drastically depends on particle size and material, many calculations must be repeated for particles which are not removed by the quality control. With a correct understanding of particle motion, the spacer can then be designed. In this design Et should satisfy the critical values reported in ref. [8].

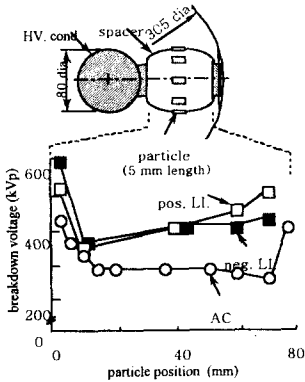


Fig. 5. Relation between breakdown voltages and particle position at 0.4 MPa.

INFLUENCE OF VOLTAGE WAVE SHAPES

Various high-voltage surges may travel in and be generated in GIS. VFT and lightning impulse voltages (LI) are typical ones. V - t characteristics for such surges have been investigated experimentally and theoretically. It was clarified that particle-initiated BDVs for VFT of oscillating frequency 2 to 20 MHz were not lower than those for LI. An example is shown in Fig. 6 [9]. Five mm long particles were attached on a 80 mm high post spacer. Open circles represent measured VFT BDVs and as solid line does measured minimum LI BDVs. It is possible to calculate V - t characteristics for LI with fairly good accuracy

by considering leader velocity. This is described as the equal voltage-time area law in eq.(3) [10],

$$\int V(t)/V_c - 1 dt = A \quad (3)$$

where V(t), applied voltage; Vc, minimum BDV; and A, voltage - time area. However, a more detailed treatment is necessary for VFT. Fig.7 shows its procedure. Each discharge process is quantitatively described in the calculation. Calculated values were plotted in Fig. 6 as solid points. They agreed well with measured ones [11].

Measurements and calculation were done for other particle lengths, other gas pressures and other VFT frequencies, and good agreement was obtained.

BDVs for other voltage waves are compared in Fig. 8. Wave form greatly influenced BDVs. Short wave front and polarity reversal resulted in low BDVs. This means that wave front as short as LI

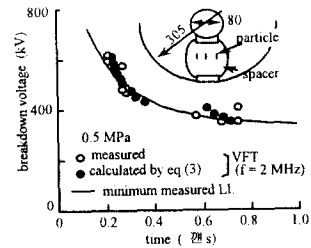


Fig. 6. Measured and calculated VFT breakdown voltages; 5mm long particles.

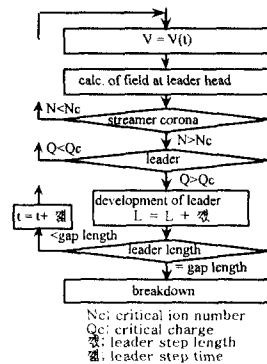


Fig. 7. Flow chart for calculation of VFT breakdown voltages.

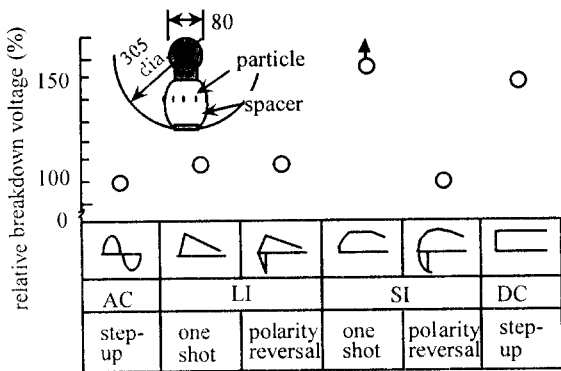


Fig. 8. Influence of voltage wave shapes of particle initiated breakdown voltages at 0.4 MPa.

is suitable for detecting foreign particles at site tests. Fig. 9 shows GIS under the site test. Oscillating LI test was introduced. The wave front was several microseconds and oscillating frequency was 100 to 300 kHz [13].

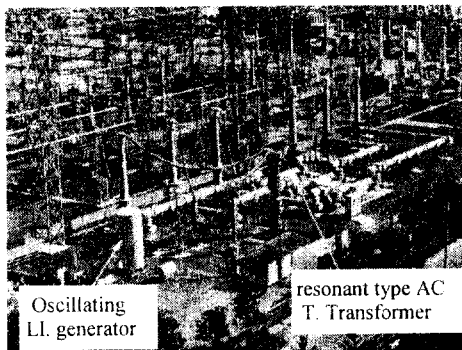


Fig. 9. Site tests with oscillating lightning impulse and AC voltages.

PARTIAL DISCHARGE DIAGNOSTIC SYSTEM BASED ON UHF METHOD

Detection of UHF electromagnetic waves emitted from PDs is superior to other methods in points of sensitivity and signal-to-noise ratio S/N and it has been studied by researchers worldwide. PDs are usually diagnosed in a frequency spectrum, and sensitivity is better than several pC [13]. To

increase diagnostic capabilities such as identification and location of PD source, time to breakdown, the degree of danger of defects and so on, it is necessary to add more functions. Fig. 10 shows an advanced UHF PD diagnostic system. A phase analysis of PD pulses in the UHF region was added to a frequency analysis, and PDs were diagnosed by using a neural network, finger print and wavelet methods. Phase spectra of PD pulses had patterns inherent to PD sources, and were helpful to get correct diagnostic results. Some spectra are shown in Fig. 11. Many spectra were acquired as a data base by changing PD sources,

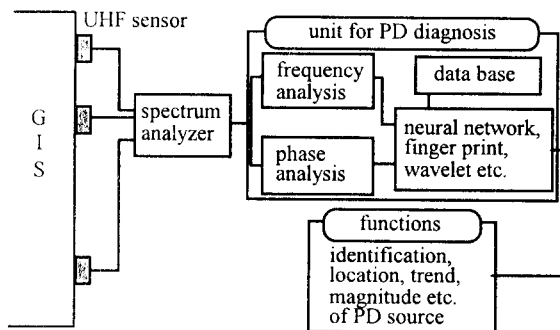


Fig. 10. UHF diagnostic system of partial discharges applying artificial intelligence.

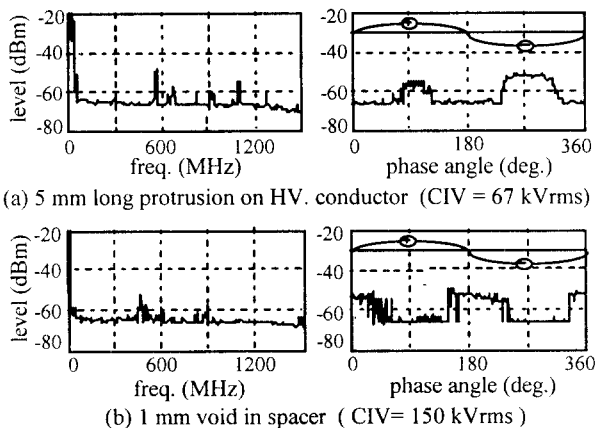


Fig. 11. Frequency and phase spectra inherent to partial discharge sources detected by the UHF method.

applied voltages, duration of voltages and, so on. With this system, the probability to get a correct answer was improved to almost 100 %.

CONCLUSIONS

Advanced insulation technologies were introduced. Points covered included breakdown from triple junctions, optimization of spacer shape, influence of particles, voltage wave effects, partial discharge diagnostic system and site tests. The newest GIS consider these points in the insulation design. Tests of full scale GIS models and prototypes confirmed the designed insulation strength and reliability.

REFERENCES

- [1] T. Yamagiwa et al., "Development of UHV gas-Insulated switchgear", Hitachi Hyoron, vol.76, p.21-26 (1994)
- [2] T. Ogawa et al., "Development of 550 kV GIS", Proc. of 8'th Annual Conf. of Power & Energy Society. IEE of Japan, no.625 (1997)
- [3] T. Hasegawa et al., "Development of insulation structure and enhancement of insulation reliability of 500 kV DC GIS", IEEE Tran. on Power Deli., vol.12, no.1, p.194-202 (1997)
- [4] F. Endo, "Gas wedge-initiated surface breakdown characteristics of epoxy rods in SF6 gas", JIEE, vol.105, no.11, p.589-596 (1985)
- [5] F. Endo, T.Yamagiwa, "Enhancement of Insulation Reliability of GIS", 1997 Japan - Korea Joint Sym. on ED and HVE, p.5 - 10.
- [6] F. Endo et al., "Development of spacer for 1000 kV GIS", 5th Annual Conf. of PES IEE of Japan, Session II, no.1413 (1994)
- [7] M. Koizumi et al., "Development of computational method for metallic particles' behavior in GIS", JASCOME 10'th Sym. on BEM's, vol.10, p.77-82 (Dec. , 1993)
- [8] F. Endo et al., "Particle-initiated breakdown characteristics and reliability improvement in SF6 gas insulation", IEEE Tran. on Power Deliv. vol.PWRD-1, no.1, p.58-65 (1986)
- [9] S. Okabe et al., "Insulation Characteristics of GIS spacer for very fast transient over-voltage", IEEE Tran. on Power Deli., vol.11, no.1, p.210-218 (Jan., 1996)
- [10] S. Okabe et al., "Voltage - time characteristics for steep front impulse voltages of particulate-contaminated spacers in SF6 gas-insulated switchgears," IEEE Trans. on Power Deliv. vol.7, no.3, p.1232 - 1238 (July, 1992)
- [11] S. Okabe et al., "V-t characteristics on GIS spacer for very fast transient overvoltages", 9'th ISH, no.2763(1995)
- [12] K.Sasaki et al., Trends of the Technology for Gas Insulated Switchgear, Hitachi Hyoron vol.70, no.8, p.839-846 (Aug.,1988)
- [13] F. Endo et al., "Insulation diagnostic system of GIS", 8'th ISH, no.66 - 01 (1993)